# The Impact of Tropical Atlantic Freshwater Fluxes on the North Atlantic Meridional Overturning Circulation

J. PAUL SPENCE AND ANDREW J. WEAVER

*School of Earth and Ocean Sciences, University of Victoria, Victoria, British Columbia, Canada*

(Manuscript received 16 June 2005, in final form 26 October 2005)

ABSTRACT

The influence of ENSO-related changes in the Atlantic-to-Pacific freshwater budget on the North Atlantic meridional overturning is examined using the University of Victoria (UVic) Earth System Climate Model. The initial analysis of freshwater fluxes in the 50-yr NCEP–NCAR (NCEP50) reanalysis product and Global Precipitation Climatology Project (GPCP) dataset reveals that the transport of water vapor out of the tropical Atlantic drainage basin is enhanced during El Niño phases and reduced during La Niña phases; a one standard deviation in the Southern Oscillation index alters the tropical Atlantic freshwater balance by about 0.09 Sv (Sv $\equiv 10^6$ m$^3$ s$^{-1}$). A weaker link with ENSO is found in the 40-yr ECMWF Re-Analysis (ERA-40), although its usefulness is severely limited by a strong and spurious trend in tropical precipitation. Model results suggest that tropical Atlantic salinity anomalies generated with the frequency and amplitude of ENSO tend not to impact deep-water formation as they are diluted en route to the North Atlantic. Lower frequency, decadal time-scale anomalies, however, do have an impact, albeit weak, on the rate of North Atlantic Deep Water formation. In addition, and contrary to earlier results, it is found that even a shift of the tropical Atlantic freshwater balance toward permanent El Niño conditions only slightly mitigates the transient reduction of North Atlantic Deep Water formation associated with the increase of anthropogenic greenhouse gases. Taken together, the results suggest that the poleward propagation of salinity anomalies from the tropical Atlantic, associated with changes in ENSO, should not be considered a significant mechanism for the variability of the North Atlantic meridional overturning in the present and foreseeable future climate.

## 1. Introduction

The transport of heat from low to high latitudes by the North Atlantic meridional overturning circulation (NAMOC) is widely recognized as a key component of Northern Hemisphere climate. Ganachaud and Wunsch (2003) estimate the present-day northward heat transport by the NAMOC to be 1.3 PW at 24°N, or roughly 70% of the global ocean meridional heat transport at that latitude. Seasonal surface cooling events, often triggered by winter storms, are important in setting up the large-scale pressure gradients, which allow for the formation of North Atlantic Deep Water (NADW) (Dickson and Brown 1994). Data based estimates of present-day NADW mass transports typically range from 15 to 22 Sv (Sv $\equiv 10^6$ m$^3$ s$^{-1}$) (Ganachaud and Wunsch 2000; Talley et al. 2003). Paleoclimate evidence linking variations in the rate of NADW formation with rapid changes in North Atlantic and European climate (Bond et al. 1993; Broecker 1997), combined with model studies demonstrating its sensitivity to surface freshwater fluxes (Stommel 1961; Manabe and Stouffer 1988; Weaver and Hughes 1992), has raised the question of potential impacts of anthropogenic forcing on the NAMOC.

The Intergovernmental Panel on Climate Change Third Assessment Report (TAR) showed that most climate models project a decrease (roughly 2–10 Sv) in the strength of the NAMOC over this century in response to increased greenhouse gas concentrations (Houghton et al. 2001). Despite differences in complexity and a wide range of responses, these models show qualitatively similar behavior; warmer sea surface temperatures and an increase in freshwater input at high latitudes from an enhanced hydrological cycle results in more stably stratified North Atlantic surface waters and reduced NADW formation. An exception discussed in

*Corresponding author address:* Dr. J. Paul Spence, School of Earth and Ocean Sciences, University of Victoria, P.O. Box 3055, Victoria, BC V8W 3P6, Canada.
E-mail: pspence@ocean.seos.uvic.ca

the TAR is the ECHAM4/Ocean Isopycnal Model (OPYC), which projected a stable NAMOC under global warming conditions. It was argued that, in this model, the local effects of warming and freshening on the surface density of the North Atlantic were mitigated by the advection of positive salinity anomalies from the tropical Atlantic (Latif et al. 2000). The salinity anomalies, in turn, were suggested to have been created by a shift in the Tropics toward more frequent El Niño conditions, which increased the amount of freshwater exported from the tropical Atlantic (Timmermann et al. 1999). Latif et al. argued that this feedback is a stronger feature in their model because it had a high meridional resolution of 0.5°N in the tropical oceans, which enabled it to better resolve tropical air–sea interactions. The results of Latif et al. (2000) highlighted the influence of ENSO on the freshwater balance of the tropical Atlantic as a possible important mechanism for NAMOC variability.

The link between ENSO and the tropical Atlantic is part of the "atmospheric bridge" described by Lau and Nath (1994). The canonical tropical Atlantic response to El Niño events is a reduction in sea level pressure, a weakening of the northeast trade winds, a northward shift in the intertropical convergence zone, and an increase in sea surface temperature north of the equator (Curtis and Hastenrath 1995; Enfield and Mayer 1997; Alexander et al. 2002). The inverse of this pattern of response holds for La Niña events. These changes lead to variations in the amount of water vapor exported from the tropical Atlantic. Schmittner et al. (2000) examined the influence of ENSO on tropical Atlantic freshwater export in a 39-yr (1958–96) National Centers for Environmental Prediction–National Center for Atmospheric Research (NCEP–NCAR) reanalysis (NCEP40) (Kalnay et al. 1996), and a 15-yr (1979–93) European Centre for Medium-Range Weather Forecasts (ECMWF) Re-Analysis (ERA-15) (Gibson et al. 1999). They found that freshwater export out of the tropical Atlantic is enhanced during El Niño events and is reduced during La Niña events by approximately 0.05–0.2 Sv (depending on the strength of the event). Using a simple zonally averaged climate model Schmittner et al. (2000) also found that permanent shifts in tropical Atlantic freshwater export in this range affected the NAMOC.

The goal of this study is to expand upon the early analysis of Schmittner et al. (2000) by performing a more extensive study of the interannual variability in the tropical Atlantic surface freshwater flux and its impact on the NAMOC. We begin by reexamining the influence of ENSO on tropical Atlantic freshwater fluxes in the most current reanalysis products in section 2. Section 3 introduces the climate model and experimental design that we employ. In section 4 we evaluate the impact of tropical Atlantic freshwater fluxes on an equilibrated climate. We determine if a reasonable increase in tropical Atlantic freshwater export, comparable to present-day El Niño conditions, mitigates the high-latitude effects on NADW formation under anthropogenic warming conditions in section 5. Conclusions are presented in section 6.

## 2. ENSO's influence on the tropical Atlantic freshwater balance

Since Schmittner et al. (2000), NCEP–NCAR has expanded its reanalysis to 57 years spanning from 1948 to 2005 (NCEP50) (Kistler et al. 2001), and ECMWF released a new 45-yr Re-Analysis (ERA-40) spanning from 1957 to 2002 (Kållberg et al. 2004). In this section we follow Schmittner et al. (2000) and reexamine the influence of ENSO on the surface freshwater balance of the tropical Atlantic drainage basin in NCEP50 and ERA-40. Precipitation ($P$) and evaporation ($E$) in these products are completely determined by the reanalysis model; no direct observations are used. Since results determined from reanalysis products should be compared with independent observational estimates, we also examine the Global Precipitation Climatology Project (GPCP) dataset (Huffman et al. 1997), which estimates $P$ by merging rain gauge and satellite observations.

We calculate surface freshwater anomalies in NCEP50 and ERA-40 from monthly mean $P - E$ fluxes at $1.9° \times 1.9°$ and $2.5° \times 2.5°$ horizontal resolution, respectively. Anomalies in GPCP are calculated from monthly mean $P$ fluxes at $2.5° \times 2.5°$ resolution. We use the observationally based Southern Oscillation index (SOI) provided by the NOAA as an index of ENSO (NOAA 2005). Very little difference was found between the NOAA SOI and the SOI calculated from reanalysis sea surface pressure anomalies at Darwin, Australia, and Papeete, Tahiti.

Figure 1 shows the times series of freshwater anomalies (when they are integrated over the Atlantic drainage basin between 20°S and 20°N) for the three datasets, along with the SOI [in units of standard deviations (SD)]. A clear correlation between the SOI and anomalies from GPCP and NCEP50 can be seen. Decreases (increases) in the SOI, tending toward El Niño (La Niña) conditions, are correlated with decreases (increases) in freshwater anomalies. The figure also reveals an unreasonable trend in ERA-40 anomalies, which is caused by a strong trend in tropical $P$ in the later years of the reanalysis. ECMWF has identified

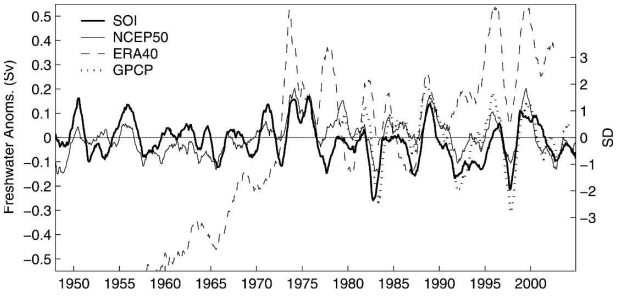


FIG. 1. Time series of the SOI (right axis) with NCEP50 and ERA-40 surface $P - E$ anomalies and surface $P$ anomalies from GPCP. The monthly anomalies were smoothed with a sliding 12-month low-pass filter and integrated over the tropical Atlantic drainage basin from 20°S to 20°N. The zonal bounds of the drainage basin are shown in Fig. 2.

the problem as stemming from errors in the analysis of humidity from satellite observations (Troccoli and Kallberg 2004). The similarity between the NCEP50 and GPCP regressions indicates that the variability is largely driven by anomalous $P$.

Table 1 shows the results of a linear regression of the SOI with the freshwater time series from Fig. 1. The correlations and slopes of the regression lines from ERA-40 show a weak and highly uncertain correlation with ENSO. This can be largely attributed to the strong $P$ trend in ERA-40. Results from NCEP50 show a weaker link to ENSO than found with GPCP. Kistler et al. (2001) note that the introduction of satellite data in 1979 dramatically improved the quality of the reanalysis. We follow their strong recommendation and evaluate NCEP50 anomalies separately for the satellite era, denoted as NCEP50_SAT. The NCEP50_SAT integrated time series nearly overlies the full-length one and is plotted independently (Fig. 3). Regression results with NCEP50_SAT anomalies compare well with GPCP and show a slightly stronger link between ENSO and tropical Atlantic freshwater fluxes than was found by Schmittner et al. (2000). They found SOI correlations of 0.65 and 0.68 and slopes of 0.06 and 0.08 for NCEP40 and ERA-15, respectively. The average total freshwater export in the Atlantic drainage basin between 20°S and 20°N determined from NCEP50_SAT is 0.23 Sv. A one SD decrease in the SOI increases this export by roughly 35%–45% according to our regression analysis.

We identify the spatial pattern of the influence of ENSO on surface freshwater fluxes in the tropical Atlantic drainage basin by linearly regressing NCEP50, NCEP50_SAT, and GPCP $P$ anomalies with the SOI at each grid point (Fig. 2). The spatial pattern and magnitudes in all three regressions are similar, with the dominance of positive signals indicating increased freshwater export under El Niño conditions. In general, they show a strong positive signal along the northeast coast of South America and weaker positive signals across the equatorial Atlantic and in the southeastern Sahel region of Africa. Negative signals are found in the northern Caribbean, the Parana–Plata basin (central Brazil), and around Lake Victoria, Africa. These results are consistent with the observed ENSO-related rainfall patterns of Giannini et al. (2000) and Rao et al. (1993) in Central and South America, of Ropelewski and Halpert (1987) and Janicot et al. (2001) in Africa, and with studies of the tropical Atlantic freshwater budget by Saravanan and Chang (2000) and Yoo and Carton (1990).

The only other significant correlation that we found between ENSO and Atlantic freshwater fluxes was between 20° and 40°N. When freshwater anomalies are integrated over this region, the NCEP50_SAT correlation with the SOI is $-0.37 \pm 0.06$ and the regression slope is $-0.018 \pm 0.04$. For GPCP, the correlation is $-0.55 \pm 0.08$ and the slope is $-0.021 \pm 0.04$. This is consistent with an extratropical link between ENSO and the Pacific–North American pattern (Giannini et al. 2001). Following El Niño events, this teleconnection results in increased $P$ in the extratropics, especially over the southeastern United States, and is essentially a weaker and anticorrelated version of ENSO's impact on the tropical Atlantic freshwater flux.

It is difficult to conclusively determine whether NCEP50 or GPCP presents the most accurate picture of ENSO's influence on the tropical Atlantic freshwater balance. The scarcity of direct rain gauge estimates in GPCP, especially over the ocean, increases the emphasis on satellite observations, which are somewhat common to GPCP and NCEP50. For example, they both include estimates of $P$ from Special Sensor Microwave Imaging and Microwave Sounding Unit satellite observations made available by NOAA. Differences between estimates based on common observations result from differences in the way that they are assimilated into the datasets. Further, conversions from satellite observations to estimates of $P$ are based on poorly understood empirical relationships between cloudiness or humidity and $P$ (Chiu et al. 1993). While differences between estimates of freshwater fluxes are the best indications of uncertainty, there is no guarantee that similarities indicate less uncertainty. We decided to focus the model results presented in this paper on NCEP50 anomalies rather than GPCP because NCEP50 covers a longer time span and freshwater fluxes are best analyzed by including the effects of both $P$ and $E$.

TABLE 1. Results of linearly regressing the SOI with integrated tropical Atlantic freshwater anomalies. Correlation coefficients, regression slopes (Sv/SD), and 95% confidence intervals were determined by linearly regressing surface freshwater anomalies integrated over the Atlantic drainage basin between 20°S and 20°N with the SOI. The time series are shown in Fig. 1 except for the NCEP50_SAT.

| Freshwater data source | Coefficient | Slope |
|---|---|---|
| ERA-40 $P - E$ September 1957–August 2002 | 0.08 ± 0.08 | 0.033 ± 0.034 |
| NCEP50 $P - E$ January 1948–December 2004 | 0.59 ± 0.05 | 0.065 ± 0.006 |
| NCEP50_SAT $P - E$ January 1979–December 2004 | 0.79 ± 0.04 | 0.087 ± 0.007 |
| GPCP $P$ January 1979–September 2004 | 0.75 ± 0.05 | 0.10 ± 0.01 |

## 3. Model description and experimental design

### a. The University of Victoria Earth System Climate Model

This study uses version 2.7 of the intermediate complexity University of Victoria Earth System Climate Model (UVic ESCM). The UVic ESCM couples a 3D ocean general circulation model, a 2D atmospheric model, a thermodynamic/dynamic sea ice model, and a land surface model. It is described in detail in Weaver et al. (2001). All components have a zonal resolution of 3.6° and a meridional resolution of 1.8°. Heat and freshwater are conserved to machine precision without the use of flux adjustments.

The ocean component is version 2.2 of the Geophysical Fluid Dynamics Laboratory Modular Ocean Model (Pacanowski 1995). The isopycnal and horizontal viscosity coefficients are set at $4.0 \times 10^2$ and $2.0 \times 10^5$ $m^2 s^{-1}$, respectively. The vertical diffusivity ranges from $3.0 \times 10^{-5}$ at the surface to $1.3 \times 10^{-4}$ $m^2 s^{-1}$ at depth according to the scheme of Bryan and Lewis (1979). Mixing associated with mesoscale eddies is parameterized according to Gent and McWilliams (1990).

The UVic ESCM employs a vertically integrated energy–moisture balance atmospheric model for computational efficiency. The underlying philosophy is that on time scales greater than a decade the ocean is a key prognostic component of the climate system (Weaver 2004). Precipitation occurs when the relative humidity exceeds 85%, and on land it is treated by a simple bucket model described in Matthews et al. (2003). Runoff occurs when a grid cell's 15-cm-deep bucket overflows and the water is returned to the ocean via weighted river discharge points. Radiative forcing associated with changes in atmospheric $CO_2$ is included as a change in the outgoing longwave radiation. The UVic ESCM is forced from start-up to equilibrium by variations in insolation and surface winds. Surface winds are prescribed from the long-term monthly mean climatology of the NCEP50 reanalysis (Kistler et al. 2001). The UVic ESCM does not simulate ENSO because there is no interannual variability in the winds due to the lack of explicit atmospheric dynamics.

The UVic ESCM has been used to investigate many scientific questions in both contemporary and paleoclimates. The model was thoroughly validated against present-day climatology in Weaver et al. (2001) and various proxy paleoreconstructions in Schmittner et al. (2002), Meissner et al. (2003), and Cottet-Puinel et al. (2004). Its computational efficiency and ability to maintain a stable climate without explicit flux adjustments permits a wide range of parameter sensitivity studies over long time scales (e.g., Wiebe and Weaver 1999; Lewis et al. 2003; Hickey and Weaver 2004).

### b. Experimental design

We investigate the influence of tropical Atlantic freshwater fluxes on the NAMOC by conducting a series of freshwater sensitivity studies initialized from an equilibrium preindustrial climate. Surface freshwater fluxes are always applied to the tropical Atlantic drainage basin between 20°S and 20°N in model year 4500. Over land, the fluxes are applied directly to river runoffs, and in the ocean they are treated as fluxes of salt. The tropical Atlantic drainage basin in the UVic ESCM does not exactly correspond to the drainage basin shown in Fig. 2 because the model has a coarser resolution. Salt is conserved in our experiments by spreading an equivalent opposing surface flux over the tropical Pacific.

We begin with a series of freshwater sensitivity studies wherein the atmospheric $CO_2$ concentration is held fixed at a preindustrial level of 280 ppm. First we evaluate the preindustrial equilibrium NAMOC in section 4a; then we gauge its sensitivity to shifts in the tropical Atlantic freshwater balance toward permanent El Niño and La Niña conditions in section 4b. In section 4c we apply sinusoidal freshwater signals of various periods to determine the frequency of variability at which NADW formation is influenced. We examine the impact of NCEP50 $P - E$ anomalies by applying them at each grid point in our forcing region in section 4d. Because we are interested in variability at interannual time scales and longer, a sliding 12-month low-pass filter is applied to the reanalysis anomalies.

In section 5 we evaluate the extent to which a shift in tropical Atlantic freshwater export toward El Niño conditions mitigates the weakening of the NAMOC under anthropogenic warming conditions. Section 5a begins

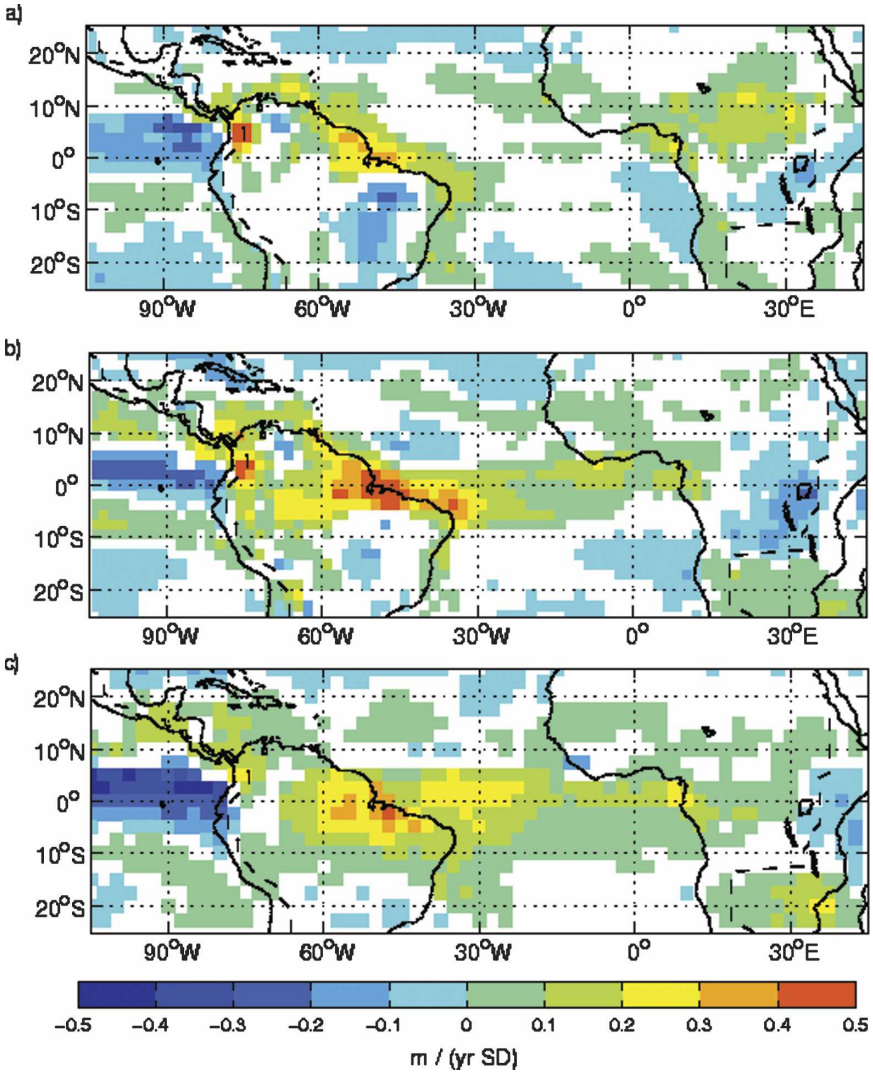


FIG. 2. The change in surface freshwater flux anomalies due to an increase in the SOI by 1 SD. (a) NCEP50 $P - E$ anomalies determined from January 1948 through December 2004. (b) NCEP50 $P - E$ anomalies determined solely from the satellite era (January 1979 through December 2004). (c) GPCP $P$ anomalies determined from January 1979 through September 2004. We linearly regress the freshwater anomalies with the SOI at each grid point and plot the slope of the regression line if its correlation coefficient exceeds the 95% confidence interval. A sliding 12-month low-pass filter is applied to the monthly anomalies prior to regression. The zonal boundary of the tropical Atlantic drainage basin, indicated by the black dashed line, was provided by A. Schmittner and was used in Schmittner et al. (2000).

by examining the NAMOC response to an exponential increase in the concentration of atmospheric $CO_2$ to 750 ppm over 250 years. We then evaluate the impact of increasing the frequency of El Niño–related tropical Atlantic freshwater fluxes. To simulate an increase in the frequency of El Niño events we identify ENSO events in the integrated NCEP50_SAT $P - E$ anomaly time series (Fig. 3). We generate four time series, each being 250 years long, by concatenating ENSO event anomalies from the gridded NCEP50_SAT data. Zeros are used as padding between the last month of one event and the first month of the next. The first series is created with 50% El Niño events and 50% La Niña events. In choosing a particular event, we chronologically cycle through the four El Niño events and three La Niña events identified in Fig. 3. For the second, third, and fourth time series we increase the number of El Niño events relative to La Niña events to 66%, 88%, and 100%, respectively. We then run model experiments with the same exponential increase in $CO_2$ and

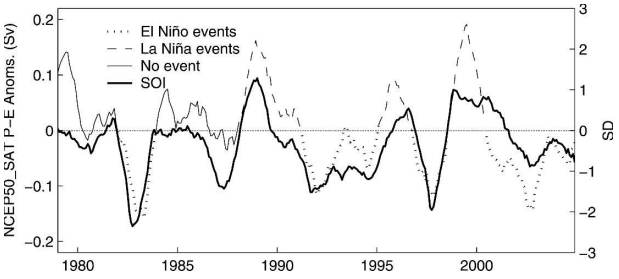


FIG. 3. Time series of the SOI and NCEP50 $P - E$ anomalies determined solely from the satellite era (January 1979–December 2004) in the same manner as the series in Fig. 1. The marked El Niño events of 1983, 1992, 1998, and 2001 along with the La Niña events of 1989, 1995, and 1999 are used to generate freshwater forcing time series with an increased frequency and amplitude of El Niño events.

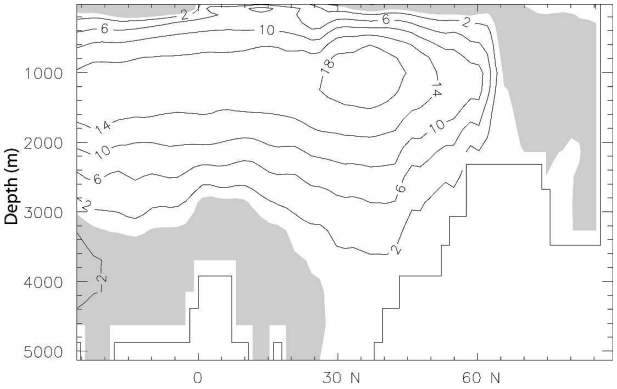


FIG. 4. Annual mean meridional overturning streamfunction (Sv) for the North Atlantic in year 4500 of CNTRL. Shaded regions are negative.

with each time series dictating the tropical Atlantic freshwater forcing. In a similar fashion, we evaluate the effect of increasing anomaly amplitudes during El Niño events in section 5b. Three more time series are generated, only this time the number of El Niño events relative to La Niña events is held fixed at 50%, and the amplitude of El Niño event anomalies are increased by 25%, 50%, and 100%.

## 4. NAMOC response to tropical Atlantic freshwater forcing with fixed $CO_2$

### *a. The preindustrial NAMOC*

The equilibrated model run, denoted CNTRL, is achieved by integrating the UVic ESCM for 4500 years with an atmospheric $CO_2$ concentration of 280 ppm (equivalent to the concentration in the year 1850). Figure 4 shows the equilibrated transport of water by the NAMOC in CNTRL. The NAMOC transport in the model is depicted by the streamfunction of the zonally integrated volume transport,

$$\Phi(\phi, z) = \int_z^0 \int_{\lambda_W}^{\lambda_E} a \cos\phi v(\lambda, \phi, z')\, d\lambda\, dz'. \qquad (1)$$

The meridional velocity $v$ is integrated over depth and from the western ($\lambda_W$) to the eastern boundary ($\lambda_E$) of the North Atlantic Ocean domain; $a$ denotes the radius of the earth. Figure 4 shows that roughly 20 Sv of the NADW formation occurs, although it has a tendency to form too far south (Weaver et al. 2001), while 2.5 Sv of Antarctic bottom water extends to about 20°N and fills the North Atlantic up to a depth of about 3000 m.

Our principal means of detecting changes in NADW formation is to examine changes in the maximum value of the NAMOC transport between the latitudinal bounds of 26° and 70°N and depths of 170 and 4000 m (NAMOC strength hereafter). CNTRL produces a reasonable equilibrium NAMOC strength of 20.5 Sv with some internal weak variability that has a dominant period of roughly 25 yr. The source of the internal variability is linked to freshwater and heat fluxes resulting from sea ice edge variability.

### *b. Response to constant forcing*

As discussed in section 2, strong ENSO events correspond to changes in tropical Atlantic freshwater export in the range of 0.1–0.2 Sv. Using a zonally averaged model, Schmittner et al. (2000) found that adding freshwater to the tropical Atlantic at a rate of 0.2 Sv, corresponding to a strong La Niña event, for 70 yr led to a collapse of the NAMOC. Under El Niño conditions of the same magnitude their NAMOC reequilibrated about 20% stronger after 70 yr. Here we evaluate the generality of their results by examining the response of the NAMOC in the more sophisticated UVic ESCM to permanent shifts in the tropical Atlantic freshwater balance.

The freshwater forcings are applied in the spatial pattern of the NCEP50_SAT regression (Fig. 2b) to simulate shifts toward El Niño and La Niña conditions. Because of this, the magnitude of our forcings is in units of SD of the SOI. A one standard deviation (1 SD) decrease is equivalent to increasing the freshwater export of the tropical Atlantic by 0.073 Sv when integrated over the forcing pattern. This is less than indicated in Table 1 because it excludes regression values outside the 95% confidence intervals.

Figure 5 shows the response of the NAMOC in the UVic ESCM to a range of constant forcings. Changes in the NAMOC begin once the tropical salinity anomalies are advected to the North Atlantic via the Gulf Stream. A 12-yr advection time scale was confirmed by passive tracers released at the mouth of the Amazon. The

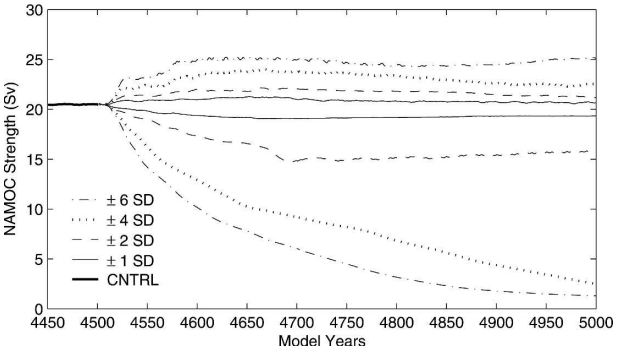


FIG. 5. Response of the NAMOC to a range of constant tropical Atlantic freshwater forcings distributed in the spatial pattern of Fig. 2b. Negative forcings correspond to El Niño conditions and strengthen the NAMOC. Positive forcings correspond to La Niña conditions and weaken the NAMOC.

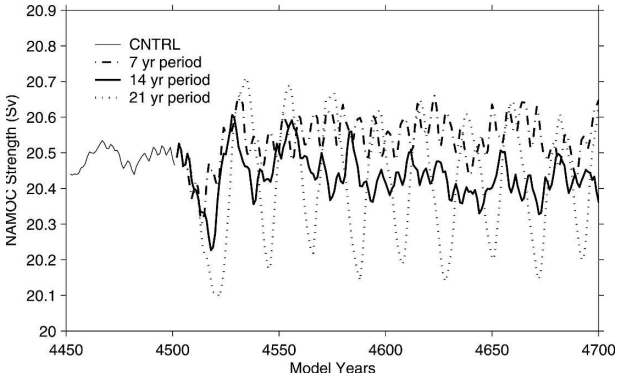


FIG. 6. NAMOC response to sinusoidal freshwater forcings distributed in the NCEP50_SAT regression pattern.

strength of the NAMOC increases (decreases) under El Niño (La Niña) conditions, as expected. The NAMOC response is observed to coincide with changes in the depth of convection in NADW formation regions.

Similar to Schmittner et al. (2000), we find the NAMOC to be more sensitive to salinity decreases than increases. For a permanent disturbance equivalent to a strong present-day El Niño event (~2 SD) the NAMOC strengthens by only 5%. Under La Niña conditions of the same magnitude the NAMOC is weakened by 25% after 500 yr. This is due to the sensitive nature of open ocean convection; while increases in surface salinity in convection regions encourages deep-water formation, decreases in salinity can actually prevent it (Weaver and Hughes 1992). The modeled convection depth in the North Atlantic stabilizes much more quickly under El Niño forcing conditions than La Niña. After 500 yr of −4 SD (0.29 Sv) forcing, equivalent to La Niña conditions twice as strong as observed, the NAMOC approaches a complete collapse. Considering that the NAMOC in Schmittner et al. (2000) collapsed after 70 yr of 0.2 Sv of forcing, we find the NAMOC to be more robust in our model.

There are a number of reasons to explain differing NAMOC sensitivities among models when similar forcings are applied. A possible candidate to account for the greater NAMOC sensitivity found in Schmittner et al. (2000) is the fact that convection and water mass sinking are coupled together (there is no horizontal structure) in zonally averaged ocean models. Further, while models often simulate similar control states of the NAMOC (they are usually tuned to meet observations), the means by which the NAMOC is maintained can vary. Significant differences in surface freshwater fluxes between models can be compensated by differences in surface heat fluxes and mixing parameterizations. Manabe and Stouffer (1999) and Schmittner and Weaver (2001) demonstrated that the stability of the NAMOC was strongly dependent upon the amount of vertical and horizontal mixing in ocean models. The intercomparison study of Gregory et al. (2005) also showed that, while the weakening of the NAMOC under warming scenarious found in most models was due primarily to changes in the surface heat flux, the relative importance of changes in the freshwater flux varied significantly. Given the large uncertainty in ocean mixing and surface flux data, it is currently not possible to quantitatively determine a real freshwater forcing threshold for the shutdown of NADW formation in the ocean.

### c. *Response to sinusoidal forcing*

Our goal in applying sinusoidal forcings is to determine if changes in the tropical Atlantic freshwater balance at the frequency and amplitude of ENSO-related variability impact NADW formation, and, if not, then to determine the frequency at which they do. The freshwater forcings are again applied in the spatial pattern of the NCEP50_SAT regression (Fig. 2b).

Figure 6 shows the NAMOC response to sinusoidal forcings with an amplitude of 2 SD of the SOI, and periods of 7, 14, and 21 yr. Considering the 7-yr period forcing, we find that, while the NAMOC response is oddly offset from the other forcing signals and the internal variability of the NAMOC is disturbed, the overall impact on the NAMOC is weak (less than 0.1 Sv). Figure 7a presents a Hovmoeller diagram of the poleward propagation of salinity anomalies for this forcing. It shows the salinity anomalies to be quickly diluted on their way to the North Atlantic with little impact outside of the forcing region. A distinct sinusoidal NAMOC response is observed for the 21-yr period forcing, with the NAMOC responding at a similar frequency to the forcing. Figure 7b shows salinity anoma-

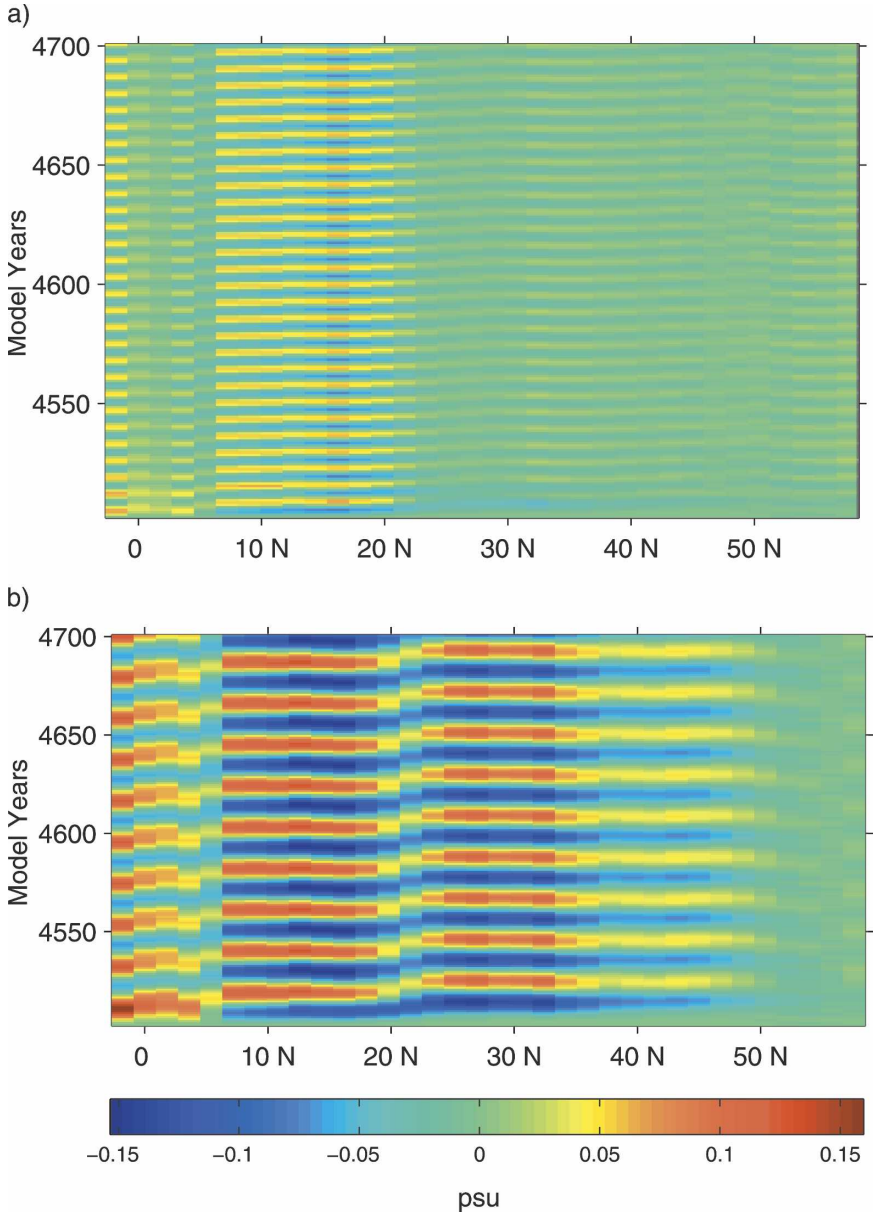


FIG. 7. Hovmoeller diagrams showing the temporal evolution of near-surface salinity anomalies as a function of latitude for (a) 7-year period and (b) 21-year period sinusoidal forcings. Anamolies were calculated annually as the difference from year 4500 of CNTRL, and then averaged both zonally and over the upper 356 m of the Atlantic Ocean.

lies at this frequency to be entrained in the subtropical gyre and persisting en route to the North Atlantic. The model response to the 14-yr period forcing is comparable to the 7-yr signal in this experiment, except for the offset from the 7-yr period NAMOC response.

We investigated the cause of this offset in another experiment wherein sinusoidal freshwater forcings were distributed evenly across the tropical Atlantic drainage basin. The amplitude of the new forcing signals was 0.15 Sv, which is equivalent to the 2-SD amplitude forcing discussed above. In this experiment the NAMOC response to the 7-yr period forcing is no longer offset from the others, and it disturbs the internal variability of the NAMOC to a lesser degree (Fig. 8). For the 14-yr period forcing a weak quasi-sinusoidal NAMOC response is observed, with a frequency comparable to the forcing. We attribute the different NAMOC response in the previous experiment to the spatial variability in the satellite-era NCEP50 regression (cf. Fig. 2b). In particular, the significant nega-

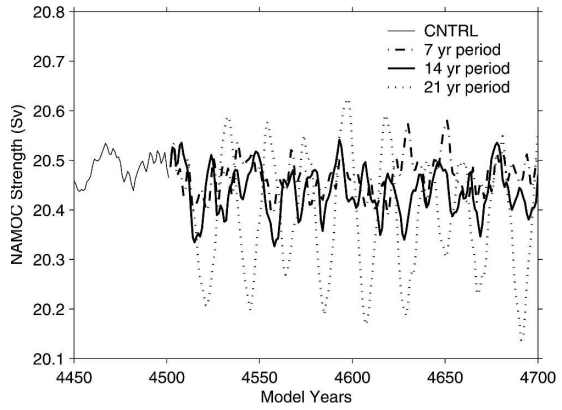


FIG. 8. Response of the NAMOC to sinusoidal tropical Atlantic freshwater forcings evenly distributed across the tropical Atlantic drainage basin between 20°N and 20°S. The amplitude of the forcing is 0.15 Sv.

tive signal located around Lake Victoria, which discharges from the Congo River basin, adds an additional mode of variability to the sinusoidal forcings that complicates the NAMOC response. The signature of this negative signal is evident around the equator in the Hovmoeller diagrams of Fig. 7b, where the competing influences of discharges from the Congo and Amazon River basins mix.

These results demonstrate the NAMOC to be sensitive to tropical Atlantic sinusoidal freshwater forcings with periods close to the advection time scale and longer. While NAMOC variability associated with freshwater forcings with the frequency and amplitude of ENSO is not significant, decadal-scale modulations of this freshwater forcing can have a weak impact on the NAMOC in the UVic ESCM (less than 0.5 Sv).

### *d. Response to NCEP50 forcing*

Here we examine the full influence of interannual tropical Atlantic surface freshwater variability on the NAMOC by applying NCEP50 $P - E$ anomalies at each grid point within the tropical Atlantic basin of the UVic ESCM. To extend the forcing signal we simply cycle through the NCEP50 anomalies for a time span of 200 years. This forcing signal is not limited to the influence of ENSO, but rather includes all modes of tropical Atlantic surface freshwater variability.

Figure 9 shows the response of the NAMOC when forced with the NCEP50 time series. We see a weak quasi-sinusoidal NAMOC response to the full-length NCEP50 forcing with a period, similar to the forcing period, that is amplified when the strength of the anomalies is doubled. The examination of the NCEP50 time series (Fig. 1) reveals the source of the decadal variability. Over the first 25 yr of the NCEP50 times series, ending just prior to the start of the major La Niña event of 1973, the flux anomalies are largely negative, with a total of $7.4 \times 10^6$ km$^3$ of freshwater exported from the basin. After 1973, a total of $9.3 \times 10^6$ km$^3$ of freshwater is added to the basin. When the model is forced by anomalies cycled over these two time periods (also shown in Fig. 9) we see the persistent influence of these freshwater biases. The NAMOC continues to strengthen when forced with anomalies cycled over the 1948/01 to 1972/12 (year/month) period, and it continues to weaken when forced with anomalies cycled over the 1973/01 to 2004/12 period. These results indicate trends in the reanalysis to be the source of the modeled decadal NAMOC variability.

We now pose the question as to whether or not the decadal trends in the reanalysis are representative of real variability in tropical Atlantic freshwater fluxes. Kistler et al. (2001) point out that the correction of coding errors after 1972, along with the introduction of satellite data in 1979, added artificial "jumps" to the reanalysis while improving its quality. This is why they strongly recommend calculating anomalies separately for the satellite era. When the ESCM is forced with NCEP50_SAT tropical Atlantic freshwater fluxes the steady-state NAMOC variability is barely disturbed (Fig. 10). It is possible that the decadal NAMOC variability modeled under the full-length NCEP50 forcing is caused by changes in the quality of the reanalysis rather than real variability in the tropical Atlantic freshwater balance.

## 5. NAMOC response to tropical Atlantic freshwater forcing with increasing $CO_2$

### *a. Response to increasing* $CO_2$ *and the frequency of El Niño events*

We now examine the NAMOC response in the UVic ESCM to anthropogenic warming conditions with an

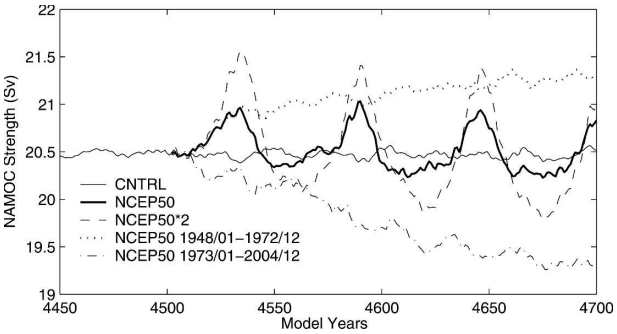


FIG. 9. The preindustrial equilibrium CNTRL run NAMOC and its response to NCEP50 $P - E$ anomalies applied at each grid point of the tropical Atlantic drainage basin and cycled for 200 yr. Results are shown for the full-length NCEP50 anomalies (January 1948 to December 2004), the full-length anomalies multiplied by a factor of 2, the first 25 yr of the full-length anomalies, and the last 32 yr.

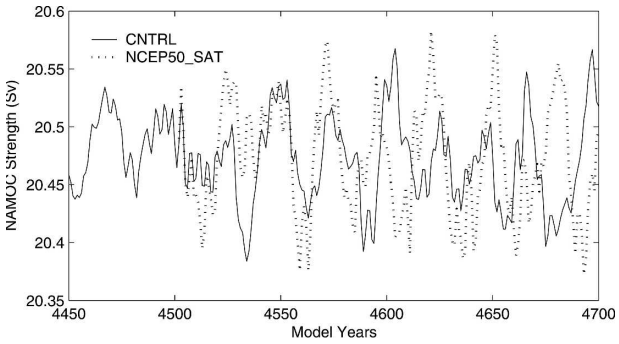


FIG. 10. As in Fig. 9 but in response to forcing from NCEP50 anomalies determined solely from the satellite era (January 1979–December 2004).

increased frequency of El Niño–related tropical Atlantic freshwater flux variability. Our objective is to corroborate the results of Latif et al. (2000), which were produced by forcing the ECHAM4/OPYC model with an exponential increase of atmospheric $CO_2$ over 250 years, according to a midrange future emission scenario (IS92A). Latif et al. (2000) attributed an increased frequency of El Niño events in their model with the production of anomalously high tropical Atlantic salinity. They further argued that, when the anomalous salinity was advected to the North Atlantic, it overwhelmed the anomalous freshwater input at high latitudes, resulting in a salinity increase in the range of 0.5–0.7 psu when averaged over the upper 375 m between 50° and 55°N, and a stable NAMOC.

Figure 11 shows the NAMOC response in a UVic ESCM run, denoted WARM, wherein we follow the IS92A scenario and exponentially increase the atmospheric $CO_2$ from 280 to 750 ppm over 250 years. The NAMOC in WARM weakens by 3.5 Sv, which places the UVic ESCM in the midrange of model responses published in the TAR (Houghton et al. 2001). A Hovmoeller diagram of salinity anomalies shows a decrease of 0.15 psu between 50° and 55°N for the WARM model run (Fig. 12a).

Also included in Fig. 11 are the NAMOC responses to WARM forcing conditions applied simultaneously with the time series of tropical Atlantic freshwater forcings that simulate an increased frequency of El Niño events. Under WARM conditions with an equal split between El Niño and La Niña events, the NAMOC response is equivalent to that observed in WARM. Increasing the number of El Niño events relative to La Niña events 66%, 88%, and 100% is found to mitigate the weakening of the NAMOC in WARM by only 14%, 23%, and 36%, respectively. The Hovmoeller diagram of salinity anomalies from the 100% El Niño events run shows that the advection of salinity from the Tropics reduces the salinity decrease observed in WARM by 0.12 psu between 50° and 55°N by the end of the run (Fig. 12b). Their remains a net decrease of 0.03 psu in the NADW formation region even when the tropical Atlantic is shifted to permanent El Niño conditions.

These results differ from those discussed in Latif et al. (2000). Significant increases in the frequency of El Niño–related tropical Atlantic freshwater forcing does not substantially mitigate the reduction of the NAMOC

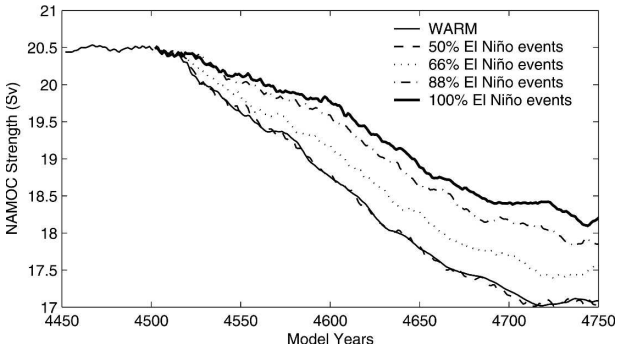


FIG. 11. Response of the NAMOC in the WARM model run, along with the NAMOC responses when the model is forced with the same $CO_2$ forcing as WARM and tropical Atlantic freshwater forcings that simulate different frequencies of El Niño events.

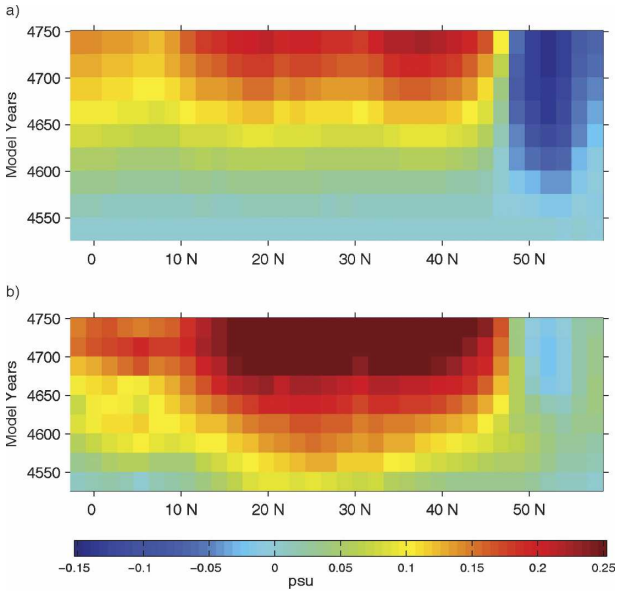


FIG. 12. Hovmoeller diagrams of the temporal evolution of near-surface salinity anomalies as a function of latitude for (a) the WARM model run and (b) the 100% El Niño events run. Salinity anomalies were calculated in the same manner as in Figs. 7a and 7b except that annually averaged salinity was recorded once every 25 years in these model runs.

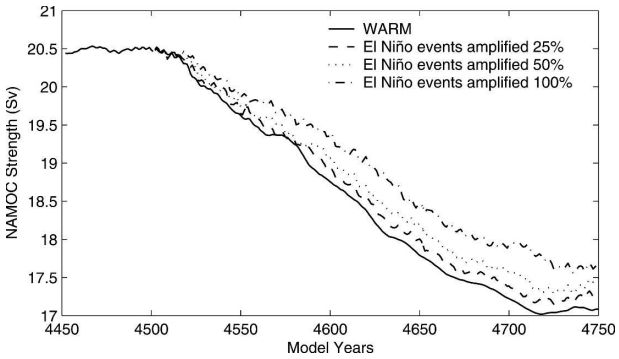


FIG. 13. As in Fig. 11 except for forcings that simulate increasing amplitudes of El Niño events.

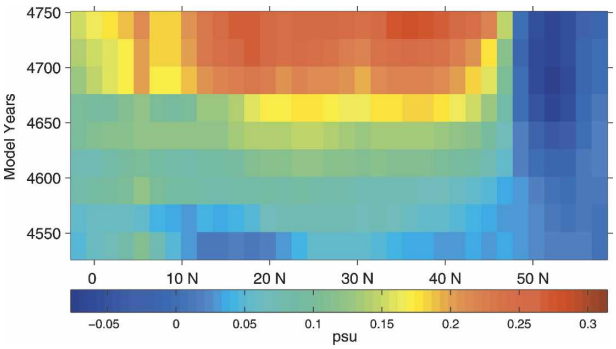


FIG. 14. As in Fig. 12 except for the 100% amplified El Niño events run.

in the UVic ESCM under anthropogenic warming conditions.

### b. *Response to increasing* $CO_2$ *and the amplitude of El Niño events*

In our final sensitivity study we examine the impact on the NAMOC of increases in the amplitude of tropical Atlantic freshwater anomalies during El Niño events under anthropogenic warming conditions. There is an equal number of El Niño and La Niña events in the freshwater forcing time series. Increasing the tropical Atlantic freshwater anomalies by 25% during El Niño events leads to a mitigation of only 7% of the weakening observed in the WARM run (Fig. 13). With a 50% and 100% increase in El Niño event anomalies the mitigation increases to 14% and 20%, respectively. The Hovmoeller diagram of ensemble-averaged salinity anomalies from the 100% amplification run shows a reduction of the salinity decrease observed in WARM of 0.09 psu between 50° and 55°N (Fig. 14).

Consistent with the results presented in section 5a, we find that significant increases in the amplitude of El Niño–related tropical Atlantic freshwater forcing does not substantially mitigate the reduction of the NAMOC in the UVic ESCM under anthropogenic warming conditions. In terms of the total freshwater forcing a 100% increase in amplitude is equivalent to increasing the frequency of El Niño to approximately 80%.

## 6. Conclusions

This study investigated interannual variability in tropical Atlantic surface freshwater flux and its impact on the NAMOC. We began by evaluating surface freshwater fluxes from ERA-40 and NCEP50 reanalysis products and the GPCP dataset. Our examination of ERA-40 revealed unreasonable trends in tropical *P* that precluded its use in this study. Results from NCEP50 and GPCP support the strong correlation, found by Schmittner et al. (2000), between ENSO and freshwater fluxes in the tropical Atlantic drainage basin. In a linear regression analysis we found that ENSO, represented by the SOI, accounted for roughly 55% of the interannual freshwater flux variability, with a 1-SD decrease in the SOI increasing the tropical Atlantic freshwater export by 0.09 Sv in NCEP50 and 0.1 Sv in GPCP.

We then used the UVic climate model to determine the impact of the northward propagation of tropical Atlantic salinity anomalies on the NAMOC equilibrated under preindustrial levels of atmospheric $CO_2$. We found that tropical Atlantic salinity anomalies generated at the frequency and amplitude of ENSO-related variability do not impact deep-water formation because they are diluted en route to the North Atlantic. However, decadal variability at the amplitude of ENSO does have a weak impact, with the rate of NADW formation increasing under El Niño conditions and decreasing under La Niña conditions by less than 5%.

Finally, we addressed the impact of an increased frequency of El Niño events under anthropogenic warming conditions on the NAMOC. Contrary to the results of Latif et al. (2000), we found that shifting the tropical Atlantic freshwater balance toward permanent El Niño conditions mitigates only 36% of the impact on deep-water formation of warming and freshening at high latitudes. Similarly, we found that doubling the amplitude of El Niño events mitigates only 20% of the high-latitude effects. Latif et al. explained their model results by noting that freshwater export in the tropical Atlantic increased by 0.3 Sv by the end of the integration due to a shift in the mean tropical climate toward El Niño conditions and an increase in the frequency of El Niño events. Estimates of the total export of freshwater from the Atlantic in the present climate range from 0.1 Sv to

0.45 Sv (Hasumi 2002). With an enhanced hydrological cycle resulting from anthropogenic warming conditions, some models predict as much as a twofold increase in this export (Zaucker and Broecker 1992). However, the majority of coupled climate models do not predict a dramatic modification of ENSO. Under $CO_2$ doubling, 3 of the 15 models examined in an intercomparison study (Merryfield 2006) exhibited statistically significant increases in ENSO amplitude, 5 exhibited significant decreases, and the ensemble average of the models presented a 5% fractional decrease in the period of ENSO. While we cannot rule out a dramatic shift in the mean state of the Tropics with anthropogenic warming, our results suggest that the poleward propagation of salinity anomalies from the tropical Atlantic owing to ENSO are unlikely to be a significant mechanism for the variability of the NAMOC in the present and foreseeable future climate.

*Acknowledgments.* This research was supported by the NSERC/CFCAS CLIVAR program. Infrastructure support from CFI, NEC, BCKDF, and UVic is also acknowledged. We are grateful to two anonymous referees for their insightful comments.

## REFERENCES

Alexander, M., I. Blade, M. Newman, J. Lanzante, N. Lau, and J. Scott, 2002: The atmospheric bridge: The influence of ENSO teleconnections on air–sea interaction over the global oceans. *J. Climate,* **15,** 2205–2231.

Bond, G., W. Broecker, S. Johnsen, J. McManus, L. Labeyrie, J. Jouzel, and G. Bonani, 1993: Correlations between climate records from North Atlantic sediments and Greenland ice. *Nature,* **365,** 143–147.

Broecker, W. S., 1997: Thermohaline circulation, the Achilles heel of our climate system: Will man-made $CO_2$ upset the current balance? *Science,* **278,** 1583–1588.

Bryan, K., and L. Lewis, 1979: Water mass model of the world ocean. *J. Geophys. Res.,* **84** (C5), 2503–2517.

Chiu, L., A. Chang, and J. Jonowiak, 1993: Comparison of monthly rain rates derived from GPI and SSM/I using probability distribution functions. *J. Appl. Meteor.,* **32,** 323–334.

Cottet-Puinel, M., A. Weaver, C. Hillaire-Marcel, A. de Vernal, P. Clark, and M. Eby, 2004: Variation of Labrador Sea water formation over the last glacial cycle in a climate model of intermediate complexity. *Quat. Sci. Rev.,* **23** (3–4), 449–465.

Curtis, S., and S. Hastenrath, 1995: Forcing of anomalous sea surface temperature evolution in the tropical Atlantic during Pacific warm events. *J. Geophys. Res.,* **100** (C8), 15 835–15 847.

Dickson, R., and J. Brown, 1994: The production of North Atlantic Deep Water: Sources, rates, and pathways. *J. Geophys. Res.,* **99** (C6), 12 319–12 341.

Enfield, D., and D. Mayer, 1997: Tropical Atlantic sea surface temperature variability and its relation to El Niño Southern Oscillation. *J. Geophys. Res.,* **102** (C1), 929–945.

Ganachaud, A., and C. Wunsch, 2000: Improved estimates of global ocean circulation, heat transport and mixing from hydrographic data. *Nature,* **408,** 453–457.

——, and ——, 2003: Large-scale ocean heat and freshwater transports during the World Ocean Circulation Experiment. *J. Climate,* **16,** 696–705.

Gent, P., and J. McWilliams, 1990: Isopycnal mixing in ocean circulation models. *J. Phys. Oceanogr.,* **20,** 150–155.

Giannini, A., Y. Kushnir, and M. Cane, 2000: Interannual variability of Carribean rainfall, ENSO, and the Atlantic Ocean. *J. Climate,* **13,** 297–311.

——, M. A. Cane, and Y. Kushnir, 2001: Interdecadal changes in the ENSO teleconnection to the Carribean region and the North Atlantic oscillation. *J. Climate,* **14,** 2867–2879.

Gibson, J. K., P. Kållberg, S. Uppala, A. Hernandez, A. Nomura, and E. Serrano, 1999: ERA-15 Description. European Centre for Medium-Range Weather Forecast Re-Analysis Project Report Series 1, 84 pp. [Available online at http://www.ecmwf.int/publications/library/do/references/list/191.]

Gregory, J., and Coauthors, 2005: A model intercomparison of changes in the Atlantic thermohaline circulation in response to increasing atmospheric $CO_2$ concentration. *Geophys. Res. Lett.,* **32,** L12703, doi:10.1029/2005GL023209.

Hasumi, H., 2002: Sensitivity of the global thermohaline circulation to interbasin freshwater transport by the atmosphere and the Bering Strait throughflow. *J. Climate,* **15,** 2516–2526.

Hickey, H., and A. J. Weaver, 2004: The Southern Ocean as a source region for tropical Atlantic variability. *J. Climate,* **17,** 3960–3972.

Houghton, J., Y. Ding, D. Griggs, M. Noguer, P. van der Linden, X. Dai, K. Maskell, and C. Johnson, Eds., 2001: *Climate Change 2001: The Scientific Basis.* Cambridge University Press, 944 pp.

Huffman, G., and Coauthors, 1997: The Global Precipitation Climatology Project (GPCP) combined precipitation dataset. *Bull. Amer. Meteor. Soc.,* **78,** 5–20.

Janicot, S., S. Trzaska, and I. Poccard, 2001: Summer Sahel-ENSO teleconnection and decadal time scale SST variations. *Climate Dyn.,* **18** (3/4), 303–320.

Kållberg, P., A. Simmons, S. Uppala, and M. Fuentes, 2004: The ERA-40 archive. European Centre for Medium Range Weather Forecast Era-40 Project Report Series 17, 34 pp. [Available online at http://www.ecmwf.int/publications/library/do/references/list/192.]

Kalnay, E., and Coauthors, 1996: The NCEP/NCAR 40-Year Reanalysis Project. *Bull. Amer. Meteor. Soc.,* **77,** 437–471.

Kistler, R., and Coauthors, 2001: The NCEP–NCAR 50-year reanalysis: Monthly means CD-ROM and documentation. *Bull. Amer. Meteor. Soc.,* **82,** 247–267.

Latif, M., E. Roeckner, U. Mikolajewicz, and R. Voss, 2000: Tropical stabilization of the thermohaline circulation in a greenhouse warming simulation. *J. Climate,* **13,** 1809–1813.

Lau, N.-C., and M. J. Nath, 1994: A modeling study of the relative roles of tropical and extratropical SST anomalies in the variability of the global atmosphere-ocean system. *J. Climate,* **7,** 1184–1207.

Lewis, J., A. Weaver, S. Johnston, and M. Eby, 2003: Neoproterozoic "snowball Earth": Dynamic sea ice over a quiescent ocean. *Paleoceanography,* **18,** 1092, doi:10.1029/2003PA000926.

Manabe, S., and R. J. Stouffer, 1988: Two stable equilibria of a coupled ocean atmosphere model. *J. Climate,* **1,** 841–866.

——, and ——, 1999: Are two modes of the thermohaline circulation stable? *Tellus,* **51A,** 400–411.

Matthews, H. D., A. J. Weaver, M. Eby, and K. J. Meissner, 2003:

Radiative forcing of climate by historical land cover change. *Geophys. Res. Lett.,* **30,** 1055, doi:10.1029/2002GL016098.

Meissner, K. J., A. Schmittner, A. J. Weaver, and J. F. Adkins, 2003: Ventilation of the North Atlantic Ocean during the Last Glacial Maximum: A comparison between simulated and observed radiocarbon ages. *Paleoceanography,* **18,** 1023, doi:10.1029/2002PA000762.

Merryfield, W., 2006: Changes to ENSO under $CO_2$ doubling in a multimodel ensemble. *J. Climate,* **19,** 4009–4027.

NOAA, cited 2005: Monthly atmospheric and sea surface temperature indices. NOAA NWS CPC. [Available online at http://www.cpc.ncep.noaa.gov/data/indices/.]

Pacanowski, R., 1995: MOM 2 documentation user's guide and reference manual. NOAA/GFDL Ocean Group Tech. Rep. 3, 232 pp.

Rao, V., M. D. Lima, and S. Franchito, 1993: Seasonal and interannual variations of rainfall over northeast Brazil. *J. Climate,* **6,** 1754–1763.

Ropelewski, C., and M. Halpert, 1987: Global and regional scale precipitation patterns associated with the El Niño/Southern Oscillation. *Mon. Wea. Rev.,* **115,** 1606–1626.

Saravanan, R., and P. Chang, 2000: Interaction between tropical Atlantic variability and El Niño–Southern Oscillation. *J. Climate,* **13,** 2177–2194.

Schmittner, A., and A. J. Weaver, 2001: Dependence of multiple climate states on ocean mixing parameters. *Geophys. Res. Lett.,* **28,** 1027–1030.

——, C. Appenzeller, and T. F. Stocker, 2000: Enhanced Atlantic freshwater export during El Niño. *Geophys. Res. Lett.,* **27,** 1163–1166.

——, K. J. Meissner, M. Eby, and A. J. Weaver, 2002: Forcing of the deep ocean circulation in simulations of the Last Glacial Maximum. *Paleoceanography,* **17,** 1015, doi:10.1029/2001PA000633.

Stommel, H., 1961: Thermohaline convection with two stable regimes of flow. *Tellus,* **13,** 224–230.

Talley, L., J. Reid, and P. Robbins, 2003: Data-based meridional overturning stream-functions for the global ocean. *J. Climate,* **16,** 3213–3226.

Timmermann, A., J. Oberhuber, A. Bacher, M. Esch, M. Latif, and E. Roeckner, 1999: Increased El Niño frequency in a climate model forced by future greenhouse warming. *Nature,* **398,** 694–697.

Troccoli, A., and P. Kållberg, 2004: Precipitation correction in the ERA-40 reanalysis. European Centre for Medium Range Weather Forecast ERA-40 Project Report Series 13, 10 pp. [Available online at http://www.ecmwf.int/publications/library/do/references/list/192.]

Weaver, A. J., 2004: The UVic Earth System Climate Model and the thermohaline circulation in past, present and future climates. *The State of the Planet: Frontiers and Challenges in Geophysics*, *Geophysical Monograph Series*, No. 150, IUGG and AGU, 279–296.

——, and T. M. Hughes, 1992: Stability and variability of the thermohaline circulation and its link to climate. *Trends in Physical Oceanography*, Research Trends Series, Vol. 1, Council of Scientific Research Integration, 15–70.

——, and Coauthors, 2001: The UVic Earth System Climate Model: Model description, climatology, and applications to past, present and future climates. *Atmos.-Ocean,* **39,** 361–428.

Wiebe, E., and A. Weaver, 1999: On the sensitivity of global warming experiments to the parameterization of sub-grid scale ocean mixing. *Climate Dyn.,* **15,** 875–893.

Yoo, J., and J. Carton, 1990: Annual and interannual variation of the freshwater budget in the tropical Atlantic Ocean and the Carribean Sea. *J. Phys. Oceanogr.,* **20,** 831–845.

Zaucker, F., and W. Broecker, 1992: The influence of atmospheric moisture transport on the freshwater balance of the Atlantic drainage basin: General circulation model simulation and observations. *J. Geophys. Res.,* **97** (D3), 2765–2773.